

1  
2 **Chapter 9:**

3 **Stratospheric ozone in the 21<sup>st</sup> century**

4  
5 D. W. Waugh<sup>1</sup>, V. Eyring<sup>2</sup>, and D. E. Kinnison,<sup>3</sup>

6  
7 <sup>1</sup> Department of Earth and Planetary Sciences, Johns Hopkins University, Baltimore, Maryland, USA.

8 <sup>2</sup> Deutsches Zentrum für Luft- und Raumfahrt, Institut für Physik der Atmosphäre, Oberpfaffenhofen,  
9 Germany.

10  
11 <sup>3</sup> National Center for Atmospheric Research, Boulder, CO, USA.

12  
13 *Corresponding Author:* D. W. Waugh ([waugh@jhu.edu](mailto:waugh@jhu.edu))

14  
15 *April 27, 2011*

1  
2  
3  
4  
5  
6  
7  
8  
9  
10  
11  
12  
13  
14  
15  
16  
17  
18  
19  
20

## TABLE OF CONTENTS

<b>9.1 INTRODUCTION</b>	<b>4</b>
<b>9.2 MODELS AND SIMULATIONS</b>	<b>5</b>
9.2.1 Chemistry-Climate Models	5
9.2.2 Simulations	7
9.2.3 Evaluation	8
<b>9.3 CHANGES IN MAJOR FACTORS AFFECTING STRATOSPHERIC OZONE.</b>	<b>10</b>
9.3.1 Stratospheric Halogens	10
9.3.2 Temperature	11
9.3.3 Transport	12
9.3.4 Other Factors	13
<b>9.4 PROJECTIONS OF THE BEHAVIOR OF OZONE</b>	<b>14</b>
9.4.1 Tropical Ozone	14
9.4.2 Mid-latitude Ozone	15
9.4.3 Spring-time Polar Ozone	16
<b>9.5 SUMMARY AND CONCLUDING REMARKS</b>	<b>18</b>
<b>9.6 REFERENCES</b>	<b>ERROR! BOOKMARK NOT DEFINED.</b>

## Abstract

This chapter discusses the future evolution of stratospheric ozone and its return to historical values from state-of-the-art three-dimensional coupled chemistry-climate models. These models have been developed by international research groups and evaluated by the atmospheric science community over the last two decades and include a detailed representation of the physical, dynamical, and chemical processes of the atmosphere, with a focus on the stratosphere. This chapter describes the models and shows examples on how these models are evaluated with observations. Factors that affect stratospheric ozone abundance, specifically ones that relate to uncertainties in the return of ozone to historical values (e.g., stratospheric halogen loading, and climate-induced temperature and transport trends) are discussed. The projected evolution of ozone is shown for different latitude regions (e.g., tropics, mid-latitudes, and polar), for different altitudes and for the total column. Hemispheric differences are also highlighted. In general models that have a better representation of transport processes measured by the models ability to represent the mean age of air and inorganic chlorine abundances are better suited to project the evolution of ozone in the 21<sup>st</sup> century. Uncertainties in current modelling approaches and recommendations for future projection simulations are also discussed.

## 9.1 Introduction

The stratospheric ozone layer has been depleted by anthropogenic emissions of halogenated species over the last decades of the 20<sup>th</sup> century. Observations show that tropospheric halogen loading is now decreasing, which reflects the controls of ozone-depleting substances (ODSs) by the Montreal Protocol and its Amendments and Adjustments (see chapter 2).<sup>1,2</sup> The total abundance of ODSs in the troposphere peaked around 1993 and has slowly declined since then. This slow decline is expected to continue over the 21<sup>st</sup> century (21C), and ODS are expected to be back to 1980 levels around 2040 and be around 1970 levels by the end of the century (see chapter 2). Atmospheric concentrations of greenhouse gases (GHGs) have also increased and are expected to further increase in the future with consequences for the ozone layer.<sup>3</sup> As a result of climate change, the ozone layer will not return to precisely its unperturbed state when the abundance of halogens returns to background levels. Furthermore, climate change complicates the attribution of ozone recovery to the decline of ODSs.

To project the future evolution of stratospheric ozone and attribute its change in response to the different forcings, numerical models are required that can adequately represent the chemistry and dynamics of the ozone layer, along with the energetics and natural variability of the atmosphere. The coupling of stratospheric chemistry with climate models has led to a new generation of models far more complex than those available when the Montreal Protocol was signed over twenty years ago. Such models, known as Chemistry-Climate Models (CCMs), are three-dimensional atmospheric circulation models with fully coupled chemistry, i.e. where chemical reactions drive changes in atmospheric composition which in turn change the atmospheric radiative balance and hence dynamics. CCMs are key tools for the detection, attribution and projection of the response of stratospheric ozone to ODSs and other factors, and allow questions about future stratospheric ozone and solar ultraviolet (UV)<sub>radiation</sub> levels to be studied. In particular, by including an explicit representation of tropospheric climate change, they make it possible to address the coupling between climate change and ozone depletion/recovery in a comprehensive manner.

Over the past decade there have been several international projects evaluating stratospheric CCMs, and related General Circulation Models (GCMs), most of which have been organized under the auspices of the WCRP's (World Climate Research Programme) SPARC (Stratospheric Processes and their Role in Climate) project. For example, the GCM-Reality Intercomparison Project (GRIPS) and the Chemistry-Climate Model Validation (CCMVal) Activity.<sup>4,5</sup> These multi-model projects have contributed directly

1 to the assessment of CCMs during the preparation of the World Meteorological Organization / United  
2 Nations Environment Programme (WMO/UNEP) Scientific Assessments of Ozone Depletion.<sup>5-10</sup>

3  
4 This chapter discusses projections of the evolution of stratospheric ozone during the 21<sup>st</sup> century. We  
5 first describe the CCMs and simulations that have been used in the last decade to project stratospheric  
6 ozone (Section 9.2). Section 9.3 briefly reviews the major factors that are affecting the ozone  
7 projections which are discussed in Section 9.4. The uncertainties and open questions in the evolution of  
8 ozone (O<sub>3</sub>) in the 21C are discussed in Section 9.5, and a summary is in Section 9.6.

## 9 **9.2 Models and Simulations**

### 11 **9.2.1 Chemistry-Climate Models**

12  
13 CCMs consist of coupled modules that calculate the dynamical fields (temperatures and winds),  
14 radiation (heating and cooling rates), and chemistry, see **Figure 9-1**. At each time step, the simulated  
15 concentrations of the radiatively active gases are used in the calculations of the net heating rates so that  
16 a change in the abundance of radiatively active gases feeds back on atmospheric dynamics fields (e.g.  
17 winds and temperature). Similarly changes in dynamics feed back on the chemical composition.

18  
19 The dynamics (i.e. the temporal evolution of wind, temperature and pressure, or other prognostic  
20 variables) in state-of-the-art CCMs is determined by solving the “primitive” equations. The basic  
21 dynamical state of the atmosphere within which transport takes place depends on a number of physical  
22 processes. These include the propagation of Rossby and gravity waves, wave-mean-flow interaction,  
23 and the diabatic circulation. Correct reproduction of the climatological mean state of the stratosphere  
24 by CCMs, including inter-hemispheric differences, inter-annual and intra-seasonal variability, is  
25 important but not sufficient: the basic dynamical mechanisms must be well represented in the  
26 underlying GCMs on which the CCMs are based if future changes are to be modeled credibly. A major  
27 issue with GCMs of the middle atmosphere is the treatment of gravity waves.<sup>4</sup> In addition, prescribed  
28 sea surface temperatures (SSTs) and sea ice concentrations (SICs) hinder the feedback between  
29 chemistry-climate interactions, so there is a need for a range of simulations looking at all aspects of the  
30 atmosphere-ocean system.

1 Radiative calculations are used in CCMs to derive photolysis rates and heating rates. Photolysis rates in  
2 the stratosphere affect the abundance of many chemical constituents that in turn control radiatively  
3 active constituents, such as O<sub>3</sub>, nitrous oxide (N<sub>2</sub>O), methane (CH<sub>4</sub>), and chlorofluorocarbons (CFCs).  
4 These radiatively active constituents are used in radiative heating calculations and therefore affect  
5 temperature and dynamics.

6

7 All CCMs used to make projections of ozone in the 21C include a comprehensive stratospheric  
8 chemistry scheme that is coupled to physical processes through the radiation calculations. This includes  
9 gas-phase and heterogeneous chemistry on aerosols and on polar stratospheric clouds (PSCs). One of  
10 the ways in which chemistry and dynamics are coupled is the temperature dependence of many  
11 chemical reaction rates. The importance of local control of ozone by chemistry relative to transport  
12 varies substantially between various times and places. In the upper stratosphere transport plays a role  
13 by controlling the concentrations of long-lived tracers such as inorganic chlorine, but photochemical  
14 timescales are so short that transport has a minimal direct impact on ozone. However, in the lower  
15 stratosphere, the photochemical timescales are longer (typically of the order of months) and  
16 interactions with dynamics are complex and more challenging to model accurately. In addition,  
17 aerosols and PSCs play an important role in chemistry of the lower stratosphere, since reactions can  
18 take place within or on the particles. In this region, heterogeneous reactions convert inorganic chlorine  
19 and bromine reservoir species to more active ozone depleting species (Chapter 4). Consequently, even  
20 though the photochemical lifetime of ozone is typically many months in the lower stratosphere, rapid  
21 chemical loss of ozone occurs when temperatures are cold, aerosols or PSCs exist, and sunlight is  
22 available (Chapter 5).

23

24 Transport in the stratosphere involves both meridional overturning (the so-called “Brewer-Dobson”  
25 circulation) and mixing. The most important aspects are the vertical (diabatic) mean motion and the  
26 horizontal mixing. Horizontal mixing is highly inhomogeneous, with transport barriers in the subtropics  
27 and at the edge of the wintertime polar vortex; mixing is most intense in the wintertime “surf zone”, i.e.  
28 the region surrounding the polar vortex, and is comparatively weak in the summertime extratropics.  
29 Accurate representation of this structure in CCMs is important for the ozone distribution itself, as well  
30 as for the distribution of chemical families and species that affect ozone chemistry, e.g. Cl<sub>y</sub>, total  
31 inorganic nitrogen (NO<sub>y</sub>), total inorganic bromine (Br<sub>y</sub>) water vapor (H<sub>2</sub>O), and CH<sub>4</sub>.

32

## 9.2.2 Simulations

CCMs have been used to perform several different types of simulations. Transient simulations consider observed or projected changes in concentrations of radiatively active gases and other boundary conditions (e.g., emissions), whereas time-slice simulations are applied to study the internal variability of a CCM under fixed conditions, e.g., GHG concentrations and SSTs, to estimate the significance of specific changes. Transient simulations are preferred for studying past and projecting future ozone changes because in these simulations, ozone responds interactively to the gradual secular trends in GHGs, ODSs, and other boundary conditions. The CCM simulations are commonly separated into “past” (or “historical”) transient simulations that are forced by observations of ODSs, GHGs, and SSTs, and are carried out to see how well the models can reproduce the past behavior of stratospheric ozone, and “future” transient simulations that are forced by trace gas projections and modeled SSTs and are carried out to make projections for the future evolution of stratospheric ozone. In addition, sensitivity or idealized simulations are performed where one or more of the forcing fields are held fixed or vary in an unrealistic manner to isolate the role of particular factors in driving changes in stratospheric O<sub>3</sub>.

In recent years the community has defined reference simulations, with a set of anthropogenic and natural forcings, to encourage consistency and comparison between simulations by different modeling groups.<sup>11,12,13</sup>

The **past reference simulation**, is defined as a transient run from 1960 to the present and is designed to reproduce the well-observed period of the last 30 years during which ozone depletion is well recorded.<sup>14</sup> This simulation examines the role of natural variability and other atmospheric changes important for ozone balance and trends. All forcings in this simulation are taken from observations. This transient simulation includes all anthropogenic and natural forcings based on changes in trace gases, solar variability, volcanic eruptions, quasi-biennial oscillation (QBO), and SSTs/SICs.<sup>13</sup>

The corresponding **future reference simulation** is a transient simulation from the past into the future (ideally 1960 to 2100) whose objective is to produce best estimates of the future ozone-climate change up to 2100 under specific assumptions about GHG increases and decreases in halogen emissions in this period. GHG concentrations (N<sub>2</sub>O, CH<sub>4</sub>, and CO<sub>2</sub>) in this reference simulation are prescribed following the Intergovernmental Panel on Climate Change Special Report on Emission Scenarios (IPCC SRES)

1 ‘A1B’ GHG scenario and surface mixing ratios of ODSs are based on the adjusted halogen scenario A1  
2 from the 2006 WMO/UNEP Assessment, which includes the earlier phase out of  
3 hydrochlorofluorocarbons (HCFCs) that was agreed to by the Parties to the Montreal Protocol in 2007,  
4 see **Figure 9-2**.<sup>2,3</sup> The future reference simulations typically include only anthropogenic forcings, and  
5 external natural forcings such as solar variability and volcanic eruptions are not considered, as they  
6 cannot be known in advance.

7 The CCMVal reference simulations have been performed by most CCM groups in support of the 2006  
8 and 2010 WMO/UNEP Assessments.<sup>2,14</sup> The first round of CCMVal (CCMVal-1) included thirteen  
9 CCMs, whereas 18 CCMs participated in the most recent second round of CCMVal (CCMVal-2), see  
10 **Table 9.1**.<sup>11</sup> In addition, several different types of **sensitivity simulations** have been performed by a  
11 small subgroup of CCMs. For example, simulations with fixed halogens have been performed to study  
12 the effect of halogens on stratospheric ozone (and climate) in a changing climate’ and ‘no greenhouse-  
13 gas induced climate change’ simulations have been performed to address the coupling of ozone  
14 depletion/recovery and climate change.<sup>15-17</sup> The SRES A1B GHG scenario is only one of several  
15 scenarios for the possible evolution of GHGs, and future simulations have also been performed using a  
16 different GHG scenarios to assess the dependence of the future ozone evolution on the GHG  
17 scenario.<sup>10,18</sup>

18

### 19 **9.2.3 Evaluation**

20

21 Confidence in, and guidance in interpreting, CCM projections of future changes in atmospheric  
22 composition can be gained by first ensuring that the CCMs are able to reproduce past observations.  
23 Limitations and deficiencies in the models can be revealed through intermodel comparisons and  
24 through comparisons with observations. As well as evaluating the simulations of the state of the  
25 atmosphere it is also important to evaluate the representation in the models of key processes that  
26 control the distribution of stratospheric ozone.<sup>5</sup> Also, with the increasing number of CCMs and the  
27 large spread in ozone projections there is a need for multi-model comparison in addition to single  
28 model studies.

29

30 Over the last decade there have been several multi-model comparisons that have evaluated different  
31 aspects of the CCMs. *Austin et al.* evaluated a mixture of time-slice and transient simulations from  
32 eight CCMs.<sup>6</sup> They focused on diagnostics to evaluate the representation of dynamics in polar regions



1 and found that many of the participating CCMs indicated a significant cold bias in high latitudes, the  
2 so-called “cold pole problem”, particularly in the southern hemisphere during winter and spring. They  
3 concluded that the main uncertainties of CCMs at that time stemmed from the performance of the  
4 underlying GCM. Cold biases have been found to exist in the stratosphere in many CCMs, consistent  
5 with that previously found for models without chemistry.<sup>4</sup>

6  
7 The thirteen CCMs that participated in CCMVal-1 were evaluated and considered in the 2006  
8 WMO/UNEP Assessment.<sup>8,19</sup> In contrast to previous studies, the CCM simulations were all transient  
9 simulations and had almost identical forcings (e.g., SSTs, GHGs, and ODSs). This eliminated many of  
10 the uncertainties in the conclusions of the earlier assessments that resulted from the differences in  
11 experimental setup of individual models. Also, and perhaps most importantly, this study was the first  
12 multi-CCM assessment to evaluate the representation of transport and distributions of important trace  
13 gases. It was shown that there were substantial quantitative differences in the simulated stratospheric  
14 Cl<sub>y</sub>, with the October mean Antarctic Cl<sub>y</sub> peak value varying from less than 2 ppb to over 3.5 ppb in the  
15 participating CCMs were found. These large differences in Cl<sub>y</sub> among the CCMs have been found to be  
16 key to diagnosing the intermodel differences in simulated ozone recovery, in particular in the Antarctic,  
17 see further discussion below.<sup>9</sup> Several other studies evaluated and analyzed different aspects in the  
18 CCMVal-1 simulations. For example, *Gettelman et al.* showed that the CCMs were able to reproduce  
19 the basic structure of the Tropical Tropopause Layer (TTL) but differences were found in cold point  
20 tropopause temperatures trends.<sup>20</sup> *Austin et al.* found that the mean model response is about 2.5% in  
21 ozone and 0.8 K in temperature during a typical solar cycle, which is at the lower end of the observed  
22 ranges of peak responses.<sup>21</sup>

23  
24 A much more extensive evaluation of CCMs was performed as part of the 2010 SPARC CCMVal  
25 Report.<sup>11</sup> This report analyzed simulations from the 18 CCMs that participated in CCMVal-2. All  
26 thirteen CCMs in CCMVal-1 participated again, but partly with updated and improved or new model  
27 versions; in addition five new models submitted output to the CCMVal archive.<sup>8</sup> The SPARC CCMVal  
28 report included evaluation of a much larger set of processes than in previous evaluations, , with an  
29 evaluation of dynamical, radiative, chemical, and transport processes as well as upper  
30 troposphere/lower stratosphere and stratosphere-troposphere coupling.<sup>8</sup> The report also included the  
31 application of observationally based performance metrics to quantify the ability of models to reproduce  
32 key processes. Overall the performance of CCMVal-2 models is similar to those in CCMVal-1. There  
33 are some diagnostics for which there is improvement (e.g., Cl<sub>y</sub>) but for other diagnostics the general

1 model performance is worse and the spread of models is larger (e.g., 100 hPa temperature and water  
2 vapor).

### 4 **9.3 Changes in major factors affecting stratospheric ozone.**

5  
6 As discussed in the Introduction, the increase in stratospheric chlorine and bromine over the last few  
7 decades was the dominant cause of decreases in O<sub>3</sub> over this period. However, as discussed in Chapter  
8 8, climate change is likely to have an increasing role in O<sub>3</sub> changes over the next century. Therefore,  
9 before discussing the projected ozone evolution, we examine the changes in the factors that control the  
10 distribution of O<sub>3</sub> as projected in the CCM simulations.

#### 12 **9.3.1 Stratospheric Halogens**

13  
14 The abundance of surface total chlorine (Cl<sub>tot</sub>) and total bromine (Br<sub>tot</sub>) peaked around 1993 and has  
15 slowly declined since then (see **Figure 9-3**).<sup>14</sup> This slow decline is expected to continue over the 21C,  
16 and ODSs are expected to be back to 1980 levels in the 2030s and be below 1970 levels by the end of  
17 century. The stratospheric chlorine and bromine loading is expected to evolve in a similar manner,  
18 although with a transport-related time delay. A commonly used variable for the effect of halogens on  
19 stratospheric ozone is the Effective Equivalent Stratospheric Chlorine (EESC).<sup>22,23</sup> The EESC is an  
20 empirical estimate of stratospheric reactive chlorine and bromine, based on measurements and  
21 projections of surface ODS, observational estimates of the transit times between the troposphere and  
22 stratosphere and the fractional release rates of different ODS. Fractional release is the fraction of  
23 inorganic halogen released from halocarbons at a given location and time. Calculations of EESC  
24 appropriate for mid-latitude lower stratosphere (mean age of air ~ 3 years) indicate a return of EESC to  
25 1980 values around 2040, while calculations for polar regions (mean age of air ~ 5.5 years) show a  
26 later return dates around 2065. There is a ~25 year difference in return dates for polar and mid-latitude  
27 EESC, even though there is only a ~2.5 year difference in mean age, because of the rapid growth of  
28 EESC around 1980 and slow decay around 2050.

29  
30 The CCMs simulate Cl<sub>y</sub> and Br<sub>y</sub> within the stratosphere, and these concentrations can be used, rather  
31 than EESC, to examine variations in halogen that effect ozone (Chapter 2). As discussed in Section 9.2,  
32 the CCM simulations use a common scenario for the surface concentrations of ODSs when making

1 projections. However, although the general evolution of Cl<sub>y</sub> and Br<sub>y</sub> is similar between CCMs, there are  
2 significant variations in the peak values of Cl<sub>y</sub> and Br<sub>y</sub> and the timing of the return to historical levels.  
3 For example, in the polar lower stratosphere the simulated peak value of Cl<sub>y</sub> in the individual CCMVal-  
4 2 models varies between 2.2 and 3.3 ppb, and the year when Cl<sub>y</sub> returns to its 1980 value varies  
5 between 2040 and 2080 (see Figure 9.13 in the SPARC CCMVal report<sup>11</sup>). These two aspects are  
6 generally related, with CCMs with lower peak Cl<sub>y</sub> values projecting an earlier return of Cl<sub>y</sub> to pre-1980  
7 values. The resulting evolution of Cl<sub>y</sub> in the CCMVal-2 multi-model mean along with its uncertainty is  
8 shown in **Figure 9-4**.

9

10 As discussed in Section 9.2.3, the observed peak Cl<sub>y</sub> in polar regions is around 3.3 ppb and most CCMs  
11 underestimate this peak value. This bias and the fact that models with lower peak return to 1980 values  
12 earlier needs to be considered when interpreting the CCM projections of ozone.

13

### 14 **9.3.2 Temperature**

15

16 As discussed in Chapter 8, changes in stratospheric temperatures can impact ozone loss by changing  
17 the rate of chemical reactions and the formation of PSCs. The stratosphere has cooled over the last four  
18 decades, and cooling is expected to continue through the 21C.<sup>9,11,24</sup> The cooling over the past few  
19 decades can be attributed to contributions from both increasing CO<sub>2</sub> and decreasing O<sub>3</sub> (the latter  
20 caused by increasing ODSs).<sup>25,26</sup> The impact of increasing CO<sub>2</sub> is expected to be dominant through the  
21 21C, and CCMs show cooling in extra-polar regions throughout the 21C. The cooling rate increases  
22 with altitude, and the projected cooling in the upper stratosphere in the 21C is around 1 K/decade  
23 (**Figure 9-5**). This cooling in the middle and upper stratosphere will decrease the rate of the gas-phase  
24 chemical reactions that destroy O<sub>3</sub> (Chapter 1, 6), and cause O<sub>3</sub> to return to historical values earlier than  
25 expected just from changes in stratospheric halogens.

26

27 In the polar lower stratosphere temperature trends could alter O<sub>3</sub> by a different mechanism; namely a  
28 cooling could lead to increase in the temporal and spatial extent of PSCs. This would increase the  
29 occurrence of heterogeneous chemical reactions that lead to ozone depletion. There are large seasonal  
30 variations in polar temperature trends, but the winter / early spring trends are most relevant for  
31 understanding polar ozone depletion. CCM projections are not uniform on whether there is a cooling or  
32 warming in either polar region, but nearly all indicate that any trends will likely be small.<sup>9,24</sup>

1 Understanding and quantifying trends in polar lower stratospheric temperatures during late winter /  
2 spring is complicated by the large year-to-year variability (especially in the northern hemisphere)  
3 which tends to interfere with any long-term trend detection. The lack of large winter trends could be  
4 due to increased downwelling and diabatic warming compensating the radiative cooling due to  
5 increasing GHGs.

### 7 **9.3.3 Transport**

8  
9 Another factor that could influence the 21C evolution of stratospheric O<sub>3</sub> is a change in stratospheric  
10 circulation. Changes in stratospheric dynamics alters the stratospheric circulation, which then impacts  
11 the O<sub>3</sub> distribution by altering the direct transport of O<sub>3</sub> among regions, as well as by altering the  
12 distribution of Cl<sub>y</sub> and Br<sub>y</sub>, and other species involved in O<sub>3</sub> destruction. A robust result of modeling  
13 studies is that an increase in GHGs leads to an increase in the tropical vertical velocities  
14 (upwelling).<sup>24,27,28</sup> This is illustrated in **Figure 9.6**, which shows the multi-model mean and variance  
15 for projections of the tropical upwelling over the 21C. When GHGs and SSTs are increased there is a  
16 significant increase in the upwelling (“REF”), whereas in a simulation with no climate change with  
17 GHG and SSTs fixed at 1960 levels, there is no change in the upwelling (“fGHG”).<sup>16</sup> The increase in  
18 tropical upwelling leads to reduced transport time scales and a decrease in the mean age of air in the  
19 stratosphere.<sup>24</sup> The CCM simulations also indicate that there has been an increase in the tropical  
20 upwelling and decrease in mean age of air over the past few decades.<sup>17,29-31</sup> However, this decrease has  
21 not been confirmed by observations, and a study by *Engel et al.* provided evidence that there has been a  
22 very small increase in the mean age of air over the last three decades.<sup>32</sup> There are however large  
23 uncertainties in the estimates of mean age from observations, and the cause of the discrepancy between  
24 the model and observations is unknown.<sup>33,34</sup>

25  
26 The impact on O<sub>3</sub> of this acceleration of the stratospheric circulation will vary between regions. For  
27 example, an increase in upwelling will decrease tropical ozone below the peak in O<sub>3</sub> concentrations  
28 (below ~10 hPa) but will increase tropical ozone above this peak. An increase in the meridional  
29 circulation will also likely increase O<sub>3</sub> in middle latitudes due to increased transport from tropical  
30 source region. We also expect the impact of changes in transport to be larger in the lower stratosphere,  
31 where photochemical timescales are longer, than in the upper stratosphere where ozone is under  
32 photochemical control.

1

### 2 **9.3.4 Other Factors**

3 The long-term evolution of O<sub>3</sub> could also be altered by changes in nitrogen and hydrogen species that  
4 are involved in ozone destruction (see Chapter 8).

5

6 Increases in tropospheric N<sub>2</sub>O are expected to occur in the 21C, leading to an increase in stratospheric  
7 NO<sub>y</sub>. This would in turn be expected to lead to a decrease in ozone in the middle and upper stratosphere  
8 due to increased O<sub>3</sub> destruction by nitrogen oxides (NO<sub>x</sub>). However, the percentage decrease in ozone is  
9 expected to be much smaller than the percentage N<sub>2</sub>O increase. The increase in NO<sub>y</sub> is smaller than  
10 N<sub>2</sub>O due to temperature decreases in the upper stratosphere.<sup>35</sup> For example, the surface concentration  
11 of N<sub>2</sub>O under scenario A1B increases by around 16% between 1980 and 2050, but the CCMs project  
12 that over the same period the stratospheric NO<sub>y</sub> generally increases by around 10% or less.

13

14 Although the increase in NO<sub>y</sub> is small over the 21C and not a dominant factor when GHGs follow the  
15 SRES A1B scenario, this is not the case for all IPCC scenarios.<sup>3</sup> For example, for the SRES A2  
16 scenario there is a larger increase in N<sub>2</sub>O, and changes related to NO<sub>y</sub> make a significant contribution to  
17 changes in upper stratospheric O<sub>3</sub> (e.g., in the GEOS CCM the decrease in O<sub>3</sub> at 3 hPa related to NO<sub>y</sub> is  
18 ~1/3 the increase related to Cl<sub>y</sub> decreases).<sup>36</sup>

19

20 The evolution of ozone in the 21C could also be affected by changes in stratospheric water vapor. An  
21 increase in water vapor would increase hydrogen oxide (HO<sub>x</sub>), and lead to increased ozone loss in the  
22 extra-polar lower and upper stratosphere, where HO<sub>x</sub> dominates ozone loss. In addition to changing  
23 HO<sub>x</sub>, an increase in water vapor would affect PSC formation and heterogeneous reactions in the  
24 CCMs, which could lead to increased spring-time polar ozone loss (see Chapter 8).

25

26 There are two mechanisms that could cause long-term increases in stratospheric H<sub>2</sub>O: (i) increases in  
27 CH<sub>4</sub>, which will lead to an increase in H<sub>2</sub>O, due to increased production from CH<sub>4</sub> oxidation, and (ii) a  
28 warming of the tropical cold-point temperature (which controls the stratospheric entry value of H<sub>2</sub>O).  
29 Surface concentrations of CH<sub>4</sub> are projected to increase over 21C, although there are large variations  
30 between GHG scenarios. Most CCMs indicate a warming of the tropical tropopause in the future,  
31 which would cause an additional increase in stratospheric H<sub>2</sub>O, by increasing the concentrations  
32 entering the stratosphere.<sup>9</sup> However, the increase in stratospheric H<sub>2</sub>O due to the warming of tropical

1 tropopause is generally smaller than contribution from a CH<sub>4</sub>.<sup>37</sup> Overall, the stratospheric global-mean  
2 water vapor trends simulated by the CCMs are small (for the A1B scenario), and are not likely a major  
3 cause of changes in stratospheric O<sub>3</sub>. This might however change, if methane increases due to the  
4 melting of permafrost is considered.

5

## 6 **9.4 Projections of the behavior of ozone**

7 The impact of the different climate factors discussed above on ozone varies between regions, both with  
8 latitude and altitude. As a consequence, the ozone evolution varies between regions. This is illustrated  
9 in **Figure 9.7**, which shows the multi-model mean change in O<sub>3</sub> between 2000 and 2100 from the  
10 CCMVal-2 models.<sup>18</sup>

### 11 **9.4.1 Tropical Ozone**

12

13 As shown in **Figure 9.7a**, the change in tropical ozone between 2000 and 2100 is very different above  
14 and below ~15 hPa. In the upper stratosphere ozone is projected to increase, whereas a decrease is  
15 projected in lower stratospheric O<sub>3</sub>.<sup>9,16</sup> This contrast is clearly seen in the solid black curves in **Figure**  
16 **9.8**, which shows the multi-model mean evolution of (a) upper and (b) lower stratospheric O<sub>3</sub> from the  
17 CCMVal-2 reference simulations.<sup>16</sup>

18

19 The different evolution of ozone in the tropical upper and lower stratosphere is due to the different role  
20 of climate change (and different role of the mechanisms discussed in Section 9.3) in the two regions.  
21 The increase in tropical upper stratosphere O<sub>3</sub> is due mainly to decreases in halogen levels, which  
22 reduces the O<sub>3</sub> loss due to catalytic chlorine and bromine reactions, and cooling due to increased  
23 GHGs, which slows the chemical reactions that destroy O<sub>3</sub>, (see Section 9.3 and Chapter 1). These two  
24 mechanisms make roughly equal contribution to the O<sub>3</sub> increase over the 21C (for the A1B GHG  
25 scenario).<sup>9,15,36,38</sup> This can be seen in Figure 9.8a by comparing the dashed (orange) and dotted (blue)  
26 curves (shaded regions), which show the projected changes in O<sub>3</sub> due to climate change and ODSs,  
27 respectively. The change due to ODSs dominates over the latter part of the 20<sup>th</sup> century, but there is a  
28 similar increase in both terms over the 21C.

29

30 In the tropical lower stratosphere the major mechanism causing long-term decreases in O<sub>3</sub> is the  
31 increase in tropical upwelling. As discussed in Section 9.3.3, a robust result in CCMs is an increase in  
32 tropical upwelling through the 21C. A future increase in upwelling in the tropics would result in a

1 faster transit of air through the tropical lower stratosphere from an enhanced Brewer-Dobson  
2 circulation which would lead to less time for production of ozone and hence lower ozone levels in this  
3 region.<sup>14</sup>

4  
5 The fact that climate change is expected to increase O<sub>3</sub> in the tropical upper stratosphere, but to  
6 decrease O<sub>3</sub> in the tropical lower stratosphere means that if, and when, O<sub>3</sub> returns to historical values  
7 (e.g., to values of O<sub>3</sub> in 1960 or 1980) varies between these altitudes. In the upper stratosphere, O<sub>3</sub> is  
8 projected to return to historical values several decades before upper stratospheric Cl<sub>y</sub> and Br<sub>y</sub> (and  
9 equivalent stratospheric chlorine, ESC; see Chapter 2) return to their historical values. For example, O<sub>3</sub>  
10 returns to 1960 values over 70 years before Cl<sub>y</sub> and Br<sub>y</sub> return to their 1960 values (see Figure 9.8a). In  
11 the tropical lower stratosphere O<sub>3</sub> may never return to historical values, even when anthropogenic  
12 ODSs have been removed from the atmosphere. For example, the multi-model mean O<sub>3</sub> decreases  
13 steadily from 1960 to 2100, even though Cl<sub>y</sub> and Br<sub>y</sub> return to 1960 values by the middle of the 21C,  
14 see Figure 9.8b.

15  
16 The evolution of tropical column ozone depends on the balance between the increase in upper  
17 stratospheric concentrations and the decrease in lower stratospheric values, and as a result the projected  
18 changes are small, see **Figure 9.9**. There is no consensus between CCMs on whether tropical column  
19 ozone will return to pre-1980 values, with some models showing O<sub>3</sub> increasing slightly above 1980  
20 values by the second half of the 21C with O<sub>3</sub> remaining below 1980 values through the 21C. There is  
21 however a consensus that tropical column ozone will not return to 1960 values, i.e. even when  
22 stratospheric halogens return to historical (pre-1960) values tropical column ozone will remain below  
23 its historical values.

#### 25 **9.4.2 Mid-latitude Ozone**

26  
27 The projected evolution of mid-latitude middle and upper stratosphere O<sub>3</sub> is very similar to that in the  
28 tropics (Figure 9.7b), with cooling in the upper stratosphere causing O<sub>3</sub> to return to historical values  
29 before Cl<sub>y</sub> and Br<sub>y</sub>. Furthermore, the magnitude of changes in O<sub>3</sub> and dates for returning to historical  
30 values are very similar to the tropics, as is the spread between CCMs. In the lower stratosphere the  
31 evolution of mid-latitude O<sub>3</sub> differs somewhat from that in the tropics. In the subtropics O<sub>3</sub> decreases  
32 but at higher latitudes (and averaged over middle latitudes) there is an increase in lower stratospheric

1 O<sub>3</sub>. As in the tropics, changes in transport play an important role in these O<sub>3</sub> changes. However, in mid-  
2 latitudes the increase in the meridional circulation leads to an increase rather than a decrease in lower  
3 stratospheric O<sub>3</sub>.<sup>38,39</sup>

4  
5 Because ozone averaged over mid-latitudes increases in the upper and lower stratosphere over the 21C,  
6 a similar evolution is projected for mid-latitude total column ozone, see Figure 9.9. The evolution of  
7 mid-latitude column ozone is similar among the CCMs, with a broad minimum around 2000 which is  
8 followed by a slow increase back to and above 1980 values. In all CCMs the return of O<sub>3</sub> to 1980  
9 values occurs before that of Cl<sub>y</sub> and Br<sub>y</sub>. However, as can be seen by the multi-model mean standard  
10 deviation that is shown in Figure 9.9, there is a spread in the magnitude of the changes and time of  
11 return to 1980 values. This spread is closely linked to the spread in simulated Cl<sub>y</sub>.<sup>7,9</sup>

12  
13 In most CCMs there are interhemispheric differences in the evolution of column ozone. The qualitative  
14 evolution is the same but there is a difference in magnitude of anomalies and in the date of return to  
15 historical values. The anomalies are larger in the SH (because of spreading of ozone hole air into  
16 midlatitudes) and the return of mid-latitude column O<sub>3</sub> to 1980 values occurs later in the SH. The  
17 difference in date of return to 1980 values appears to be due to interhemispheric difference in changes  
18 in transport. The increase in stratospheric circulation driven by climate change transports more O<sub>3</sub> into  
19 NH midlatitude lower stratosphere than SH.<sup>38</sup>

### 21 **9.4.3 Spring-time Polar Ozone**

22  
23 The largest ozone depletion is observed in the polar lower stratosphere during spring, especially in the  
24 Antarctic (see Chapter 5). As a result a major focus of model simulations is the projected evolution of  
25 polar lower stratospheric ozone during spring.

#### 26 *Antarctic.*

27  
28 All models project a qualitatively similar evolution for Antarctic (60°-90°S) ozone in spring, with a  
29 broad minimum around 2000 followed by a very slow increase and a return to 1980 values sometime  
30 around the middle of the century, see **Figure 9.10b**. There are however, as in the extrapolar regions,  
31 significant quantitative differences among the models, including a wide spread in the minimum values  
32 around 2000 and dates when ozone returns to 1980 (or 1960) values.<sup>7,9</sup>



1  
2  
3  
4  
5  
6  
7  
8  
9  
10  
11  
12  
13  
14  
15  
16  
17  
18  
19  
20  
21  
22  
23  
24  
25  
26  
27  
28  
29  
30  
31  
32

Several different ozone indices have been used to quantify variations in Antarctic ozone, including the polar cap average (Figure 9.10), ozone mass, daily minimum ozone, and area of the ozone hole (area of ozone less than 220 DU).<sup>40</sup> There are some differences in the evolution of these different diagnostics, in particular over the 2000 to 2030 period where the rate of change varies. However, all diagnostics show the same broad evolution with return to 1980 values around the middle of century, and a wide spread among the models in quantitative details.

The evolution of Antarctic spring ozone is dominated by the changes in Cl<sub>y</sub> and Br<sub>y</sub>, and changes in climate (temperature and transport) are not, in general, a major factor. This can be seen by the very close correspondence of the evolution of ozone and Cl<sub>y</sub> (or ESC),<sup>7,9,16</sup>. The spread in Antarctic ozone projections are, as a result, primarily due to differences in simulated Cl<sub>y</sub> (and Br<sub>y</sub>) among the models. Models that simulate a smaller peak Cl<sub>y</sub> have an earlier return of Cl<sub>y</sub> to 1980 values, and generally also have smaller ozone depletion and earlier return of ozone to 1980 values. This relationship suggests that the low bias in Cl<sub>y</sub> in most models results in an early bias in the projected return of ozone to 1980 values, i.e., the return to 1980 values will likely occur later than indicated by the multi-model mean shown in Figure 9.10b.

Projections of the recovery of the Antarctic ozone hole have also been made using parametric models based on estimates of EESC and analyzed polar temperatures.<sup>41</sup> These calculations indicate that the ozone hole area will remain constant until around 2015, and then decrease to zero around 2070. This recovery date is later than that simulated by most models (see Figure 9b of *Eyring et al.* [2007]), but this difference is consistent with a bias in the models dynamics and transport.<sup>9</sup>

#### *Arctic.*

Dynamical effects play a much larger role in the evolution of springtime Arctic ozone than in the Antarctic, and as a consequence there is large interannual variability. This interannual variability is much larger than the long-term changes, and time series need to be filtered (smoothed) to see long-term trends. However, long-term evolution of the filtered Arctic ozone is qualitatively the same as in other regions: There is a broad minimum around 2000 with slow increase over the first half of the 21C, see Figure 9-10a.

1 Although there is qualitative agreement among the models there are large quantitative variations in the  
2 simulated changes in Arctic ozone, with some models showing only a small or even no change in ozone  
3 while others show a large response to changes in halogens. There are substantial variations among the  
4 models in the date when ozone returns 1980 values (2020 to 2060), e.g., see Figure 16 of *Austin et al.*  
5 [2010].<sup>7</sup>

6  
7 An early study by *Shindell et al.* projected a substantial increase in Arctic ozone depletion, and the  
8 development of an Arctic ozone hole, because of climate change.<sup>42</sup> However, subsequent studies have  
9 not reproduced this result. Even though there is a large spread among the CCMs, in both CCMVal-1  
10 and CCMVal-2, none of the CCMs predict large Arctic ozone decreases in the future.

11  
12 Models project that Arctic ozone will return to 1980 values before Antarctic ozone, with the difference  
13 varying from only a few years in some models to over 25 years in others. The evolution of Cl<sub>y</sub> and Br<sub>y</sub>  
14 is similar in both polar regions, but because changes in temperature and transport play a significant role  
15 in the Arctic, the evolution of Arctic O<sub>3</sub> does not follow that of Cl<sub>y</sub> and Br<sub>y</sub> as closely as Antarctic  
16 ozone. In particular, acceleration of the Brewer-Dobson circulation and increases in polar temperatures  
17 cause an earlier return than that expected just because of changes in halogens.<sup>43</sup> These dynamical  
18 changes vary substantially among models, and as a consequence so does the differences in return dates  
19 of Arctic and Antarctic ozone.

20

## 21 **9.5 Summary and Concluding Remarks**

22

23 The evolution of stratospheric ozone in the 21<sup>st</sup> century will depend not only on changes (expected  
24 decreases) in the abundance of stratospheric halogens but also on changes due to increases in well-  
25 mixed greenhouse gases. The latter will cool the stratosphere, increase the abundance of nitrogen and  
26 hydrogen species involved in ozone destruction, and may also alter transport within the stratosphere.  
27 The impact of the greenhouse-gas-induced change on ozone varies between regions, and as a  
28 consequence the ozone evolution will vary between regions.

29

30 In the upper stratosphere the projected ozone evolution is very similar in the tropics and middle  
31 latitudes, with ozone increasing back to 1960 values in the first 2-3 decades of the 21<sup>st</sup> century. This  
32 rapid increase in ozone is due to both decreases in ODSs and cooling due to increased GHGs. The

1 evolution in the mid-latitude lower stratosphere is similar to that in the upper stratosphere, although  
2 climate-change induced increases in the circulation play more of a role than cooling. In the tropical  
3 lower stratosphere the evolution is, however, very different: here ozone decreases throughout the 21<sup>st</sup>  
4 century due to climate-change-induced increases in the tropical upwelling. In the Antarctic, the models  
5 consistently show a broad minimum near year 2000 followed by a slower return to 1980 values than in  
6 middle latitudes (with the return delayed until the middle of the century). In the Arctic, the interannual  
7 variability in ozone is larger than long-term trends and the models are less consistent in their  
8 representation of ozone recovery. However, in most models Arctic ozone returns to 1980 values before  
9 Antarctic ozone.

10

11 Although there is generally qualitative agreement among models in the evolution of ozone there are  
12 some substantial quantitative differences. In particular there is a wide spread in projected ozone values  
13 at specified periods and in the dates when ozone returns to historical values. In many cases the  
14 differences among model projections can be related to differences in the simulated  $Cl_y$ , and improving  
15 the transport of  $Cl_y$ , which will reduce the uncertainty in ozone projections, is a remaining major  
16 challenge.

17

18 It is also important to note that the ozone projections depend on scenarios for surface concentrations of  
19 ODSs and GHGs, and the majority of the projections have considered very similar ODS scenarios and  
20 the same GHG scenario. However, a recent examination of CCM projections for six different GHG  
21 scenarios found that lower GHG emissions result in (i) smaller reductions in ozone in the tropical lower  
22 stratosphere (due to smaller increases in tropical upwelling) and (ii) smaller increases in upper  
23 stratospheric ozone globally (due to less severe stratospheric cooling).<sup>10</sup> Largest differences among the  
24 six GHG scenarios were found over northern midlatitudes (~20 DU by 2100) and in the Arctic (~40  
25 DU by 2100) with divergence mainly in the second half of the 21st century. The results suggest that  
26 effects of GHG emissions on future stratospheric ozone should be considered in climate change  
27 mitigation policy and ozone projections should be assessed under more than a single GHG scenario.

28

29 Future assessments should also consider the uncertainty in how the models force the organic halogen  
30 lower boundary condition. Currently, projections of future organic halogen loadings are based on  
31 projected emission rates and an estimate of the global atmospheric lifetime of each organic halogen.  
32 These factors are then used to create time-dependent volume mixing ratio lower boundary conditions,  
33 that are then used to force the CCMs. However, the destruction of each halogen in the CCMs is

1 dependent on the tropical upwelling, meridional mixing, and chemical loss rates (e.g., photolysis rates),  
2 and the CCM-derived halogen lifetimes can be very different from the lifetimes assumed for the given  
3 projection scenario. By forcing all CCMs to use fixed mixing ratio lower boundary conditions, the flux  
4 into the tropical lower stratosphere is fixed in all the models. This will minimize the spread in model  
5 derived ozone return dates.<sup>44</sup> If models were forced with flux lower boundary conditions, the simulated  
6 ODS would be consistent with the simulated loss of ODSs and any changes in the model circulation  
7 would also feedback on these loss rates. Models with a more realistic circulation (e.g., representation of  
8 mean age) would also more accurately represent the fractional release of inorganic halogens from their  
9 parent organic. This approach would give a more accurate representation of ozone depletion and  
10 recovery.

11

12 Another consideration for future simulations is inclusion of interactive ocean and sea ice modules in  
13 the CCMs. In all but one of the CCM simulations discussed above the sea surface temperatures and sea  
14 ice concentrations were prescribed, and the important coupling between the atmosphere and oceans /  
15 cyrosphere are not represented. The one exception is the Canadian Middle Atmosphere Model  
16 (CMAM), in which the atmospheric model is coupled to an ocean / sea ice model<sup>45</sup>. Inclusion of these  
17 couplings in the CCMs leads to a more complete representation of the climate system and feedbacks,  
18 which could be particularly important for simulations of stratospheric polar ozone and its impact on  
19 tropospheric climate.

20

## 21 **Acknowledgements**

22 We acknowledge the Chemistry-Climate Model Validation (CCMVal) Activity of the World Climate  
23 Research Programme's (WCRP) Stratospheric Processes and their Role in Climate (SPARC) project  
24 for organizing and coordinating the model data analysis, and the British Atmospheric Data Centre  
25 (BADC) for collecting and archiving the CCMVal model output. We thank Anne Douglass for a  
26 careful review of this chapter and Irene Cionni and Luke Oman for preparing some of the figures. This  
27 research was supported by the US National Science Foundation and by the German Aerospace Center  
28 (DLR).

29

## 2 9.6 References

3

41 Montzka, S. A., J. H. Butler, B.D. Hall, D. J. Mondeel, and J. W. Elkins, A decline in tropospheric  
5 bromine, *Geophys. Res. Lett.*, *30*, 1826, doi:10.1029/2003GL017745, 2003.

62 World Meteorological Organization (WMO)/United Nations Environment Programme (UNEP),  
7 Scientific Assessment of Ozone Depletion: 2006, World Meteorological Organization, Global Ozone  
8 Research and Monitoring Project, Report No. 50, Geneva, Switzerland, 2007.

93 Intergovernmental Panel on Climate Change (IPCC) (2000), Special Report on Emissions Scenarios: A  
10 Special Report of Working Group III of the Intergovernmental Panel on Climate Change, 599 pp.,  
11 Cambridge Univ. Press, Cambridge, U. K.

12

134 Pawson, S., K. Kodera, K. Hamilton, T. G. Shepherd, S. R. Beagley, B. A. Boville, J. D. Farrara, T. D.  
14 A. Fairlie, A. Kitoh, W. A. Lahoz, U. Langematz, E. Manzini, D. H. Rind, A. A. Scaife, K. Shibata, P.  
15 Simon, R. Swinbank, L. Takacs, R. J. Wilson, J. A. Al-Saadi, M. Amodei, M. Chiba, L. Coy, J. de  
16 Grandpré, R. S. Eckman, M. Fiorino, W. L. Grose, H. Koide, J.N. Koshyk, D. Li, J. Lerner, J. D.  
17 Mahlman, N. A. McFarlane, C. R. Mechoso, A. Molod, A. O'Neill, R. B. Pierce, W. J. Randel, R. B.  
18 Rood, and F. Wu, The GCM-Reality Intercomparison Project for SPARC: Scientific Issues and Initial  
19 Results, *Bull. Am. Meteorol. Soc.*, *81*, 781-796, 2000.

20

215 Eyring V., N.R.P. Harris, M. Rex, T.G. Shepherd, D.W. Fahey, G.T. Amanatidis, J. Austin, M.P.  
22 Chipperfield, M. Dameris, P.M. De F. Forster, A. Gettelman, H.F. Graf, T. Nagashima, P.A. Newman,  
23 S. Pawson, M.J. Prather, J.A. Pyle, R.J. Salawitch, B.D. Santer, and D.W. Waugh, A strategy for  
24 process-oriented validation of coupled chemistry-climate models. *Bull. Am. Meteorol. Soc.*, *86*, 1117–  
25 1133, 2005a.

266 Austin, J., D. Shindell, S. R. Beagley, C. Brühl, M. Dameris, E. Manzini, T. Nagashima, P. Newman,  
27 S. Pawson, G. Pitari, E. Rozanov, C. Schnadt, and T. G. Shepherd, Uncertainties and assessments of  
28 chemistry-climate models of the stratosphere, *Atmos. Chem. Phys.*, *3*, 1-27. 2003.

297 Austin, J., J. Scinocca, D. Plummer, L. Oman, D. Waugh, H. Akiyoshi, S. Bekki, P. Braesicke, N.  
30 Butchart, M. P. Chipperfield, D. Cugnet, M. Dameris, S. Dhomse, V. Eyring, S. Frith, R. Garcia, H.  
31 Garny, A. Gettelman, S.C. Hardiman, D. Kinnison, J. F. Lamarque, E. Mancini, M. Marchand, M.  
32 Michou, O. Morgenstern, T. Nakamura, S. Pawson, G. Pitari, J. Pyle, E. Rozanov, T. G. Shepherd, K.  
33 Shibata, H. Teyssedre, R.J. Wilson, and Y. Yamashita, The decline and recovery of total column ozone  
34 using mult-model time series analysis, *J. Geophys. Res.*, doi:10.1029/2010JD013857, 2010.

35

368 Eyring, V., N. Butchart, D. W. Waugh, H. Akiyoshi, J. Austin, S. Bekki, G. E. Bodeker, B. A. Boville,  
37 C. Brühl, M. P. Chipperfield, E. Cordero, M. Dameris, M. Deushi, V. E. Fioletov, S. M. Frith, R. R.  
38 Garcia, A. Gettelman, M. A. Giorgetta, V. Grewe, L. Jourdain, D. E. Kinnison, E. Mancini, E. Manzini,  
39 M. Marchand, D. R. Marsh, T. Nagashima, P. A. Newman, J. E. Nielsen, S. Pawson, G. Pitari, D. A.  
40 Plummer, E. Rozanov, M. Schraner, T. G. Shepherd, K. Shibata, R. S. Stolarski, H. Struthers, W. Tian,  
41 and M. Yoshiki, Assessment of temperature, trace species and ozone in chemistry-climate model  
42 simulations of the recent past, *J. Geophys. Res.*, *111*, D22308, doi:10.1029/2006JD007327, 2006.

439 Eyring, V., D. W. Waugh, G. E. Bodeker, E. Cordero, H. Akiyoshi, J. Austin, S. R. Beagley, B.  
44 Boville, P. Braesicke, C. Brühl, N. Butchart, M. P. Chipperfield, M. Dameris, R. Deckert, M. Deushi,

- 1 S. M. Frith, R. R. Garcia, A. Gettelman, M. Giorgetta, D. E. Kinnison, E. Mancini, E. Manzini, D. R.  
2 Marsh, S. Matthes, T. Nagashima, P. A. Newman, J. E. Nielsen, S. Pawson, G. Pitari, D. A. Plummer,  
3 E. Rozanov, M. Schraner, J. F. Scinocca, K. Semeniuk, T. G. Shepherd, K. Shibata, B. Steil, R.  
4 Stolarski, W. Tian, and M. Yoshiki, Multimodel projections of stratospheric ozone in the 21st century,  
5 *J. Geophys. Res.*, 112, D16303, doi:10.1029/2006JD008332, 2007.
- 610 Eyring, V., I. Cionni, J. F. Lamarque, H. Akiyoshi, G. E. Bodeker, A. J. Charlton-Perez, S. M. Frith,  
7 A. Gettelman, D. E. Kinnison, T. Nakamura, L. D. Oman, S. Pawson, and Y. Yamashita, Sensitivity of  
8 21st century stratospheric ozone to greenhouse gas scenarios, *Geophys. Res. Lett.*, 37, L16807,  
9 doi:10.1029/2010GL044443, 2010b.
- 1011 SPARC CCMVal (2010), SPARC Report on the Evaluation of Chemistry-Climate Models, V. Eyring,  
11 T. G. Shepherd, D. W. Waugh (Eds.), SPARC Report No. 5, WCRP-132, WMO/TD-No. 1526,  
12 <http://www.atmosp.physics.utoronto.ca/SPARC>.
- 1312 Eyring, V., D. E. Kinnison, and T. G. Shepherd, Overview of planned coupled chemistry-climate  
14 simulations to support upcoming ozone and climate assessments, *SPARC Newsletter No. 25*, 11–17,  
15 2005b.
- 1613 Eyring, V., M. P. Chipperfield, M. A. Giorgetta, D. E. Kinnison, E. Manzini, K. Matthes, P. A.  
17 Newman, S. Pawson, T. G. Shepherd, and D. W. Waugh, Overview of the New CCMVal Reference  
18 and Sensitivity Simulations in Support of Upcoming Ozone and Climate Assessments and the Planned  
19 SPARC CCMVal Report, *SPARC Newsletter No. 30*, p.20-26, 2008.
- 2014 World Meteorological Organization (WMO)/United Nations Environment Programme (UNEP),  
21 Scientific Assessment of Ozone Depletion: 2010, World Meteorological Organization, Global Ozone  
22 Research and Monitoring Project, Report No. 52, Geneva, Switzerland, 2011.
- 2315 Waugh, D. W., L. Oman, S. R. Kawa, R. S. Stolarski, S. Pawson, A. R. Douglass, P. A. Newman, and J.  
24 E. Nielsen, Impacts of climate change on stratospheric ozone recovery, *Geophys. Res. Lett.*, 36,  
25 L03805, doi:10.1029/2008GL036223, 2009.
- 2616 Eyring, V., I. Cionni, G. E. Bodeker, A. J. Charlton-Perez, D. E. Kinnison, J. F. Scinocca, D. W.  
27 Waugh, H. Akiyoshi, S. Bekki, M. P. Chipperfield, M. Dameris, S. Dhomse, S. M. Frith, H. Garny, A.  
28 Gettelman, A. Kubin, U. Langematz, E. Mancini, M. Marchand, T. Nakamura, L. D. Oman, S. Pawson,  
29 G. Pitari, D. A. Plummer, E. Rozanov, T. G. Shepherd, K. Shibata, W. Tian, P. Braesicke, S. C.  
30 Hardiman, J. F. Lamarque, O. Morgenstern, D. Smale, J. A. Pyle, and Y. Yamashita, Multi-model  
31 assessment of stratospheric ozone return dates and ozone recovery in CCMVal-2 models, *Atmos.*  
32 *Chem. Phys.*, 10, 9451-9472, doi:10.5194/acp-10-9451-2010, 2010a.
- 3317 Garcia, R. R., and W. J. Randel, Acceleration of the Brewer-Dobson Circulation due to Increases in  
34 Greenhouse Gases, In Press *J. Atmos. Sci.* **65**, 2731-2739, 2008.
- 3518 Oman, L. D., D. A. Plummer, D. W. Waugh, J. Austin, J. F. Scinocca, A. R. Douglass, R. J. Salawitch,  
36 T. Canty, H. Akiyoshi, S. Bekki, P. Braesicke, N. Butchart, M. P. Chipperfield, D. Cugnet, S. Dhomse,  
37 V. Eyring, S. Frith, S.C. Hardiman, D.E. Kinnison, J.-F. Lamarque, E. Mancini, M. Marchand, M.  
38 Michou, O. Morgenstern, T. Nakamura, J. E. Nielsen, D. Olivie, G. Pitari, J. Pyle, E. Rozanov, T. G.  
39 Shepherd, K. Shibata, R. S. Stolarski, H. Teyssedre, W. Tian, Y. Yamashita, and J. R. Ziemke, Multi-  
40 model assessment of the factors driving stratospheric ozone evolution over the 21st century, *J.*  
41 *Geophys. Res.*, 115, D24306, doi:10.1029/2010JD014362, 2010.
- 4219 Waugh, D. W., and V. Eyring, Quantitative performance metrics for stratospheric-resolving chemistry-  
43 climate models, *Atmos. Chem. Phys.*, 8, 5699-5713, 2008.

- 120 Gettelman, A., T. Birner, V. Eyring, H. Akiyoshi, S. Bekki, C. Brühl, M. Dameris, D. E. Kinnison, F.  
 2 Lefevre, F. Lott, E. Mancini, G. Pitari, D. A. Plummer, E. Rozanov, K. Shibata, A. Stenke, H.  
 3 Struthers, and W. Tian, The Tropical Tropopause Layer 1960–2100, *Atmos. Chem. Phys.*, 9, 1621-  
 4 1637, 2009.
- 521 Austin, J., K. Tourpali, E. Rozanov, H. Akiyoshi, S. Bekki, G. Bodeker, C. Brühl, N. Butchart, M.  
 6 Chipperfield, M. Deushi, V. I. Fomichev, M. A. Giorgetta, L. Gray, K. Kodera, F. Lott, E. Manzini, D.  
 7 Marsh, K. Matthes, T. Nagashima, K. Shibata, R. S. Stolarski, H. Struthers, and W. Tian, Coupled  
 8 chemistry climate model simulations of the solar cycle in ozone and temperature, *J. Geophys. Res.*,  
 9 113, D11306, 2008.
- 1022 Daniel, J. S., S. Solomon, R. W. Portmann, R. R. Garcia, Stratospheric ozone destruction: The  
 11 importance of bromine relative to chlorine. *J. Geophys. Res.*, 104, 23,871-23,880, 1999.
- 1223 Newman, P. A., J. S. Daniel, D. W. Waugh, and E. R. Nash, A new formulation of equivalent effective  
 13 stratospheric chlorine (EESC), *Atmos. Chem. Phys.*, 7, 4537-4552, 2007.
- 1424 Butchart, N., I. Cionni, V. Eyring, T. G. Shepherd, D. W. Waugh, H. Akiyoshi, J. Austin, C. Bruhl, M.  
 15 P. Chipperfield, E. Cordero, M. Dameris, R. Deckert, S. Dhomse, S. M. Frith, R. R. Garcia, A.  
 16 Gettelman, M. A. Giorgetta, D. E. Kinnison, F. Li, E. Mancini, C. McLandress, S. Pawson, G. Pitari,  
 17 D. A. Plummer, E. Rozanov, F. Sassi, J. F. Scinocca, K. Shibata, B. Steil, and W. Tian, Chemistry-  
 18 climate model simulations of 21st century stratospheric climate and circulation changes, *J. Climate*, 23,  
 19 5349-5374, doi: 10.1175/2010JCLI3404.1, 2010.
- 2025 Shepherd, T. G., and A. I. Jonsson, On the attribution of stratospheric ozone and temperature changes to  
 21 changes in ozone-depleting substances and well-mixed greenhouse gases, *Atmos. Chem. Phys.*, 8, 1435-  
 22 1444, 2008.
- 2326 Stolarski, R. S., A. R. Douglass, P. A. Newman, S. Pawson, and M. R. Schoeberl, Relative contribution  
 24 of greenhouse gases and ozone-depleting substances to temperature trends in the stratosphere: a  
 25 chemistry/climate model study, *J. Climate*, 23, 28-42, 2010.
- 2627 Butchart, N., A. A. Scaife, M. Bourqui, J. de Grandpré, S. H. E. Hare, J. Kettleborough, U. Langematz,  
 27 E. Manzini, F. Sassi, K. Shibata, D. Shindell, and M. Sigmond, Simulations of anthropogenic change in  
 28 the strength of the Brewer-Dobson circulation, *Clim. Dyn.*, doi:10.1007/s00382-006-0162-4, 2006.
- 2928 Butchart, N., and A. A. Scaife, Removal of chlorofluorocarbons by increased mass exchange between  
 30 the stratosphere and the troposphere in a changing climate, *Nature*, 410, 799-802, 2001.
- 3129 Austin, J., J. Wilson, F. Li, and H. Vomel, Evolution of Water Vapor Concentrations and Stratospheric  
 32 Age of Air in Coupled Chemistry-Climate Model Simulations, *J. Atmos. Sci.*, 64, 905-921, 2007.
- 3330 Oman, L., D. W. Waugh, S. Pawson, R. S. Stolarski, and P. A. Newman (2009a), On the influence of  
 34 anthropogenic forcings on changes in the stratospheric mean age, *J. Geophys. Res.*, 114, D03105,  
 35 doi:10.1029/2008JD010378, 2009.
- 3631 McLandress, C., and T. G. Shepherd, Simulated Anthropogenic Changes in the Brewer-Dobson  
 37 Circulation, Including Its Extension to High Latitudes, *J. Clim.*, 22, doi 10.1175/2008JCLI2679.1, 2008.
- 3832 Engel, A., et al., Age of stratospheric air unchanged within uncertainties over the past 30 years, *Nature*  
 39 *Geosciences*, 2, 28 – 31, 2009.
- 4033 Waugh, D. W., Atmospheric dynamics: The age of stratospheric air, *Nature Geosciences*, 2, 14 – 16,  
 41 2009.
- 4234 Garcia, R. R., W. J. Randel, and D. E. Kinnison, On the determination of age of air trends from  
 43 atmospheric trace species, *J. Atm. Sci.*, pp139-154, Vol68, doi: 10.1175/2010JAS3527.1, 2011.

- 135 Rosenfield, J.E., and A.R. Douglass, Doubled CO<sub>2</sub> effects on NO<sub>y</sub> in a coupled 2-D model, *Geophys. Res. Lett.* 25, 4381-4384, 1998.
- 336 Oman, L., D.W. Waugh, S.R. Kawa, R. S. Stolarski, A.R. Douglass, and P.A. Newman, Mechanisms and feedbacks causing changes in upper stratospheric ozone in the 21st century, *J. Geophys. Res.*, 115, D05303, doi:10.1029/2009JD012397, 2010.
- 637 Oman, L., D. W. Waugh, S. Pawson, R. S. Stolarski, and J. E. Nielsen (2008), Understanding the changes of stratospheric water vapor in coupled chemistry-climate model simulations, *J. Atmos. Sci.*, 65, 3278– 3291, doi:10.1175/2008JAS2696.1, 2008.
- 938 Shepherd, T. G., Dynamics, Stratospheric Ozone, and Climate Change. *Atmos. Ocean*, 46, 117-138, 2008.
- 1139 Li, F., R.S. Stolarski, and P.A. Newman, Stratospheric ozone in the post-CFC era, *Atmos. Chem. Phys.*, 9, 2207-2213, 2009.
- 1340 Bodeker, G. E., H. Shiona, and H. Eskes, Indicators of Antarctic ozone depletion, *Atmos. Chem. Phys.*, 5, 2603-2615, 2005.
- 1541 Newman, P. A., E. R. Nash, S. R. Kawa, S. A. Montzka, and S. M. Schauffler, When will the Antarctic ozone hole recover?, *Geophys. Res. Lett.*, 33, L12814, doi:10.1029/2005GL025232, 2006.
- 1742 Shindell, D.T., D. Rind, P. Lonergan, Increased polar stratospheric ozone losses and delayed eventual recovery owing to, *Nature*, 392, 589-592, 1998.
- 1943 Austin, J., and F. Li, On the relationship between the strength of the Brewer-Dobson circulation and the age of stratospheric air, *Geophys. Res. Lett.*, 33, L17807, doi:10.1029/2006GL026867, 2006.
- 2144 Douglass, A. R., R. S. Stolarski, M. R. Schoeberl, C. H. Jackman, M. L. Gupta, P. A. Newman, J. E. Nielsen, and E. L. Fleming, Relationship of loss, mean age of air and the distribution of CFCs to stratospheric circulation and implications for atmospheric lifetimes, *J. Geophys. Res.*, 113, D14309, doi:10.1029/2007JD009575, 2008.
- 2545 McLandress, C., A. I. Jonsson, D. A. Plummer, M. C. Reader, J. F. Scinocca, and T. G. Shepherd, Separating the dynamical effects of climate change and ozone depletion: Part 1. Southern Hemisphere Stratosphere. *J. Climate*, 23, 5002–5020, doi: 10.1175/2010JCLI3586.1, 2010.
- 2846 Austin, J., and R.J. Wilson, Sensitivity of polar ozone to sea surface temperatures and chemistry, *J. Geophys. Res.*, 115, D18303, doi:10.1029/2009JD013292, 2010.
- 3047 Lamarque J.-F., D. E. Kinnison, P. G. Hess, F. M. Vitt (2008), Simulated lower stratospheric trends between 1970 and 2005: Identifying the role of climate and composition changes, *J. Geophys. Res.*, 113, D12301, doi:10.1029/2007JD009277, 2008.
- 3348 Akiyoshi, H., L. B. Zhou, Y. Yamashita, K. Sakamoto, M. Yoshiki, T. Nagashima, M. Takahashi, J. Kurokawa, M. Takigawa, and T. Imamura, A CCM simulation of the breakup of the Antarctic polar vortex in the years 1980-2004 under the CCMVal scenarios, *J. Geophys. Res.*, 114, D03103, doi:10.1029/2007JD009261, 2009.
- 3749 Scinocca, J. F., N. A. McFarlane, M. Lazare, J. Li and D. Plummer, Technical Note: The CCCma third generation AGCM and its extension into the middle atmosphere, *Atmos. Chem. Phys.*, 8, 7055-7074, 2008.
- 4050 deGrandpre, J., S. R. Beagley, V. I. Fomichev, E. Griffioen, J. C. McConnell, A. S. Medvedev and T. G. Shepherd, Ozone climatology using interactive chemistry: Results from the Canadian Middle Atmosphere Model, *J. Geophys. Res.*, 105, 26475-26491, 2000.



- 151 Déqué, M., Frequency of precipitation and temperature extremes over France in an anthropogenic  
2 scenario: model results and statistical correction according to observed values. *Global and Planetary*  
3 *Change*, 57, 16-26, 2007.
- 452 Teysse re H., M. Michou, H. L. Clark, B. Josse, F. Karcher, D. Olivie, V.-H. Peuch, D. Saint-Martin,  
5 D. Cariolle, J.-L. Atti , P. N d lec, P. Ricaud, V. Thouret, R. J. van der A, A. Volz-Thomas, and F.  
6 Cheroux, A new tropospheric and stratospheric Chemistry and Transport Model MOCAGE-Climat for  
7 multi-year studies: evaluation of the present-day climatology and sensitivity to surface processes,  
8 *Atmos. Chem. Phys.*, 7, 5815-5860, 2007.
- 953 Stenke, A., M. Dameris, V. Grewe, and H. Garny, Implications of Lagrangian transport for simulations  
10 with a coupled chemistry-climate model, *Atmos. Chem. Phys.*, 9, 5489-5504, 2009.
- 1154 Garny, H., M. Dameris, and A. Stenke, Impact of prescribed SSTs on climatologies and long-term  
12 trends in CCM simulations, *Atmos. Chem. Phys.*, 9, 6017-6031, 2009.
- 1355 J ckel, P., Tost, H., Pozzer, A., Br hl, C., Buchholz, J., Ganzeveld, L., Hoor, P., Kerkweg, A.,  
14 Lawrence, M. G., Sander, R., Steil, B., Stiller, G., Tanarhte, M., Taraborrelli, D., van Aardenne, J., and  
15 Lelieveld, J.: The atmospheric chemistry general circulation model ECHAM5/MESSy1: consistent  
16 simulation of ozone from the surface to the mesosphere, *Atmos. Chem. Phys.*, 6, 5067– 5104, 2006.
- 1756 Pawson, S., R. S. Stolarski, A. R. Douglass, P. A. Newman, J. E. Nielsen, S. M. Frith, and M. L. Gupta,  
18 Goddard Earth Observing System chemistry-climate model simulations of stratospheric ozone-  
19 temperature coupling between 1950 and 2005, *J. Geophys. Res.*, 113, D12103,  
20 doi:10.1029/2007JD009511, 2008.
- 2157 Jourdain, L., S. Bekki, F. Lott, and F. Lef vre, The coupled chemistry-climate model LMDz-  
22 REPROBUS: description and evaluation of a transient simulation of the period 1980–1999, *Annales*  
23 *Geophysicae*, 26, 6, 1391-1413, 2008.
- 2458 Shibata, K. and M. Deushi, Long-term variations and trends in the simulation of the middle atmosphere  
25 1980-2004 by the chemistry-climate model of the Meteorological Research Institute, *Annales*  
26 *Geophysicae*, 26, 1299-1326, 2008a.
- 2759 Shibata, K. and M. Deushi, Simulation of the stratospheric circulation and ozone during the recent past  
28 (1980-2004) with the MRI chemistry-climate model, CGER's Supercomputer Monograph Report  
29 Vol.13, National Institute for Environmental Studies, Japan, 154 pp, 2008b.
- 3060 Schraner, M., E. Rozanov, C. Schnadt-Poberaj, P. Kenzelmann, A. Fischer, V. Zubov, B. P. Luo, C.  
31 Hoyle, T. Egorova, S. Fueglistaler, S. Br nnimann, W. Schmutz and T. Peter, Technical Note:  
32 Chemistry-climate model SOCOL: version 2.0 with improved transport and chemistry/ microphysics  
33 schemes, *Atmos. Chem. Phys.*, 8, 5957-5974, doi:10.5194/acp-8-5957-2008, 2008.
- 3461 Egorova, T., E. Rozanov, V. Zubov, E. Manzini, W. Schmutz, and T. Peter, Chemistry-climate model  
35 SOCOL: a validation of the present-day climatology, *Atmos. Chem. Phys.*, 5, 1557-1576, 2005.
- 3662 Pitari G., E. Mancini, V. Rizi and D. T. Shindell: Impact of Future Climate and Emission Changes on  
37 Stratospheric Aerosols and Ozone, *J. Atmos. Sci.*, 59, 2002.
- 3863 Austin, J., and N. Butchart, Coupled chemistry-climate model simulations of the period 1980-2020:  
39 Ozone depletion and the start of ozone recovery, *Q. J. R. Meteorol. Soc.*, 129, 3225-3249, 2003.
- 4064 Tian, W, and M. P. Chipperfield, A new coupled chemistry-climate model for the stratosphere: the  
41 importance of coupling for future O<sub>3</sub>-climate predictions, *Quart J. Roy. Meteor. Soc.*, 131, pp281-303,  
42 2005.

- 165 Tian, W., M. P. Chipperfield, L. J. Gray, and J. M. Zawodny, Quasi-biennial oscillation and tracer  
2 distributions in a coupled chemistry-climate model, *J. Geophys. Res.*, 111, D20301,  
3 doi:10.1029/2005JD006871, 2006.
- 466 Morgenstern, O., P. Braesicke, M. M. Hurwitz, F. M. O'Connor, A. C. Bushell, C. E. Johnson, and J. A.  
5 Pyle, The World Avoided by the Montreal Protocol, *Geophys. Res. Lett.*, 35, L16811,  
6 doi:10.1029/2008GL034590, 2008.
- 767 Morgenstern, O., P. Braesicke, F. M. O'Connor, A. C. Bushell, C. E. Johnson, S. M. Osprey, and J. A.  
8 Pyle, Evaluation of the new UKCA climate-composition model. Part 1: The stratosphere. *Geosci.*  
9 *Model Dev.*, 1, 43-57, 2009.
- 1068 Garcia R. R., D. R. Marsh, D. E. Kinnison, B. A. Boville, and F. Sassi, Simulation of secular trends in  
11 the middle atmosphere, 1950–2003, *J. Geophys. Res.*, 112, D09301, doi:10.1029/2006JD007485, 2007.

12

13

14

15

16

17

18

19

1 **Table 9-1.** CCMs that are used for ozone projections in the CCMVal-2 intercomparison of SPARC  
 2 CCMVal [2010]: name of the model, group and references for model documentations.

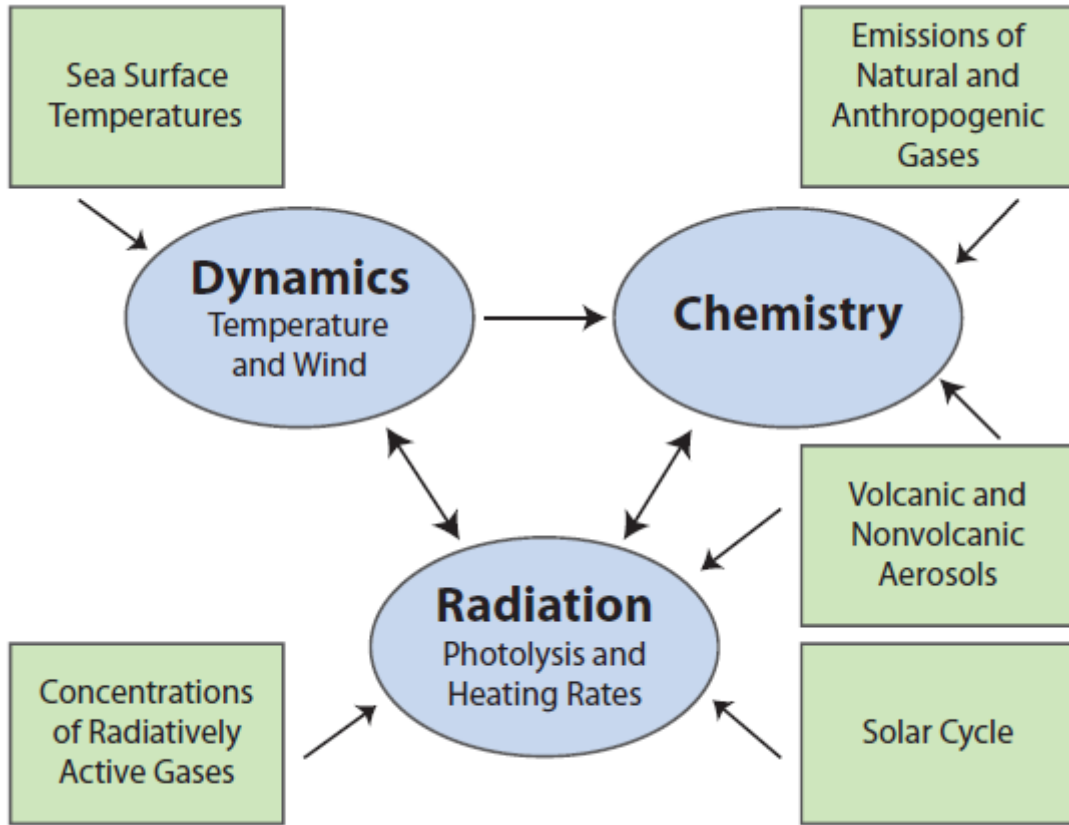
3

	<b>CCM</b>	<b>Group and Location</b>	<b>References</b>
1	AMTRAC3	GFDL, USA	<i>Austin and Wilson</i> [2010] <sup>46</sup>
2	CAM3.5	NCAR, USA	<i>Lamarque et al.</i> [2008] <sup>47</sup>
3	CCSRNIES	NIES, Tokyo, Japan	<i>Akiyoshi et al.</i> [2009] <sup>48</sup>
4	CMAM	MSC, University of Toronto, York Univ., Canada	<i>Scinocca et al.</i> [2008] <sup>49</sup> ; <i>deGrandpre et al.</i> [2000] <sup>50</sup>
5	CNRM-ACM	Meteo-France; France	<i>Déqué</i> [2007] <sup>51</sup> ; <i>Teyssède et al.</i> [2007] <sup>52</sup>
6	E39CA	DLR, Germany	<i>Stenke et al.</i> [2009] <sup>53</sup> ; <i>Garny et al.</i> [2008] <sup>54</sup>
7	EMAC	MPI Mainz, Germany	<i>Jöckel et al.</i> [2006] <sup>55</sup>
8	GEOSCCM	NASA/GSFC, USA	<i>Pawson et al.</i> [2008] <sup>56</sup>
9	LMDZrepro	IPSL, France	<i>Jourdain et al.</i> [2008] <sup>57</sup>
10	MRI	MRI, Japan	<i>Shibata and Deushi</i> [2008a,b] <sup>58,59</sup>
11	NIWA-SOCOL	NIWA, NZ	<i>Schraner et al.</i> [2008] <sup>60</sup> ; <i>Egorova et al.</i> [2005] <sup>61</sup>
12	SOCOL	PMOD/WRC and ETHZ, Switzerland	<i>Schraner et al.</i> [2008] <sup>60</sup> ; <i>Egorova et al.</i> [2005] <sup>61</sup>
13	ULAQ	University of L'Aquila, Italy	<i>Pitari et al.</i> [2002] <sup>62</sup> ; <i>Eyring et al.</i> [2006; 2007] <sup>8,9</sup>
14	UMETRAC	NIWA, NZ	<i>Austin and Butchart</i> [2003] <sup>63</sup>
15	UMSLIMCAT	University of Leeds, UK	<i>Tian and Chipperfield</i> [2005] <sup>64</sup> ; <i>Tian et al.</i> , [2006] <sup>65</sup>
16	UMUKCA-METO	MetOffice, UK	<i>Morgenstern et al.</i> [2008, 2009] <sup>66,67</sup>
17	UMUKCA-UCAM	University of Cambridge, UK	<i>Morgenstern et al.</i> [2008, 2009] <sup>66,67</sup>
18	WACCM	NCAR, USA	<i>Garcia et al.</i> [2007] <sup>68</sup>

4  
 5  
 6

1 FIGURES

2  
3  
4



5  
6  
7  
8  
9  
10  
11  
12  
13  
14

**Figure 9-1.** Schematic of a Chemistry-Climate Model (CCM). The core of a CCM (oval symbols) consists of an general circulation model (GCM) that includes calculation of the heating and cooling rates and a detailed chemistry module. They are interactively coupled. Photolysis rates are calculated online or are determined from a lookup table. Arrows indicate the direction of effect. Rectangular boxes denote external impacts. From Figure 5.1 of *WMO* [2007].<sup>2</sup>

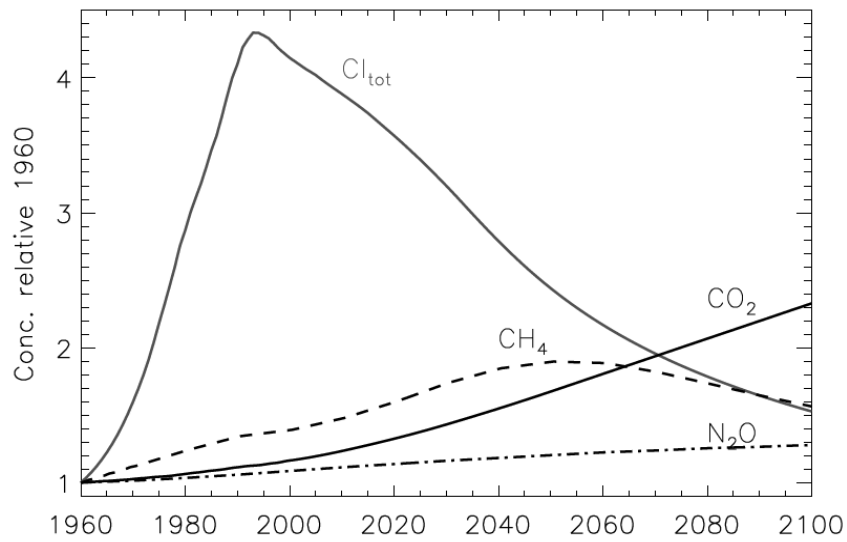
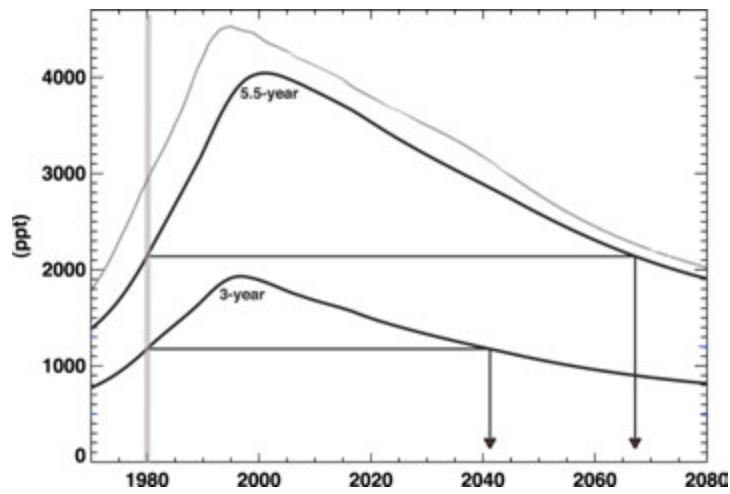


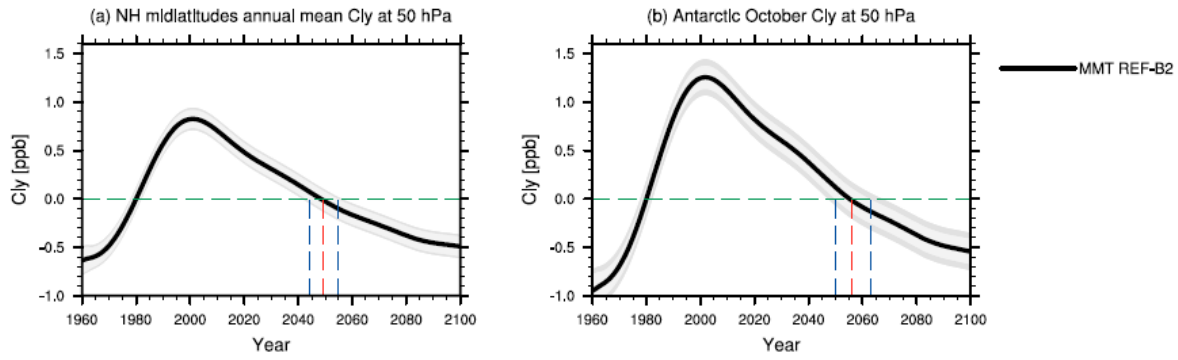
**Figure 9-2.** Time series of the surface concentrations of total chlorine from the WMO (2007) scenario, and GHGs from the IPCC SRES A1B scenario.<sup>2,3</sup> Concentrations are shown relative to their 1960 concentrations (820 ppt for Cl<sub>tot</sub>, 1265 ppb for CH<sub>4</sub>, 316 ppm for CO<sub>2</sub>, and 291 ppb for N<sub>2</sub>O).

1  
2  
3  
4  
5  
6  
7  
8



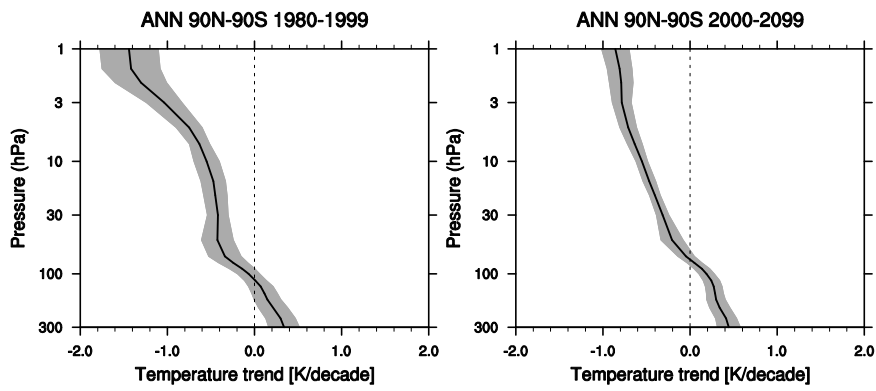
1  
2  
3  
4  
5  
6  
7  
8  
9  
10

**Figure 9-3.** Evolution of surface  $Cl_{tot}+60Br_{tot}$  (gray curve) and EESC for mean age-of-air values of 3 and 5.5 years (black curves) for WMO [2002] ODS scenarios. The gray vertical line indicates the reference year of 1980. The black horizontal and vertical lines indicate the recovery date of EESC to 1980 values. From Figure 5 of *Newman et al.* [2007].<sup>23</sup>



1  
 2 **Figure 9-4.** 1980 baseline-adjusted multi-model trend estimates of annually averaged inorganic  
 3 chlorine ( $Cl_y$ ) at 50 hPa (ppb) for **(a)** annual northern midlatitude mean 35–60°N and **(b)** Antarctica  
 4 (60°S–90°S) in October. The red vertical dashed line indicates the year when the multi-model trend in  
 5  $Cl_y$  returns to 1980 values and the blue vertical dashed lines indicate the uncertainty in these return  
 6 dates. Multi-model mean derived from Figures 3.6 and 3.11 of *WMO* [2011].<sup>14</sup>

7  
 8  
 9

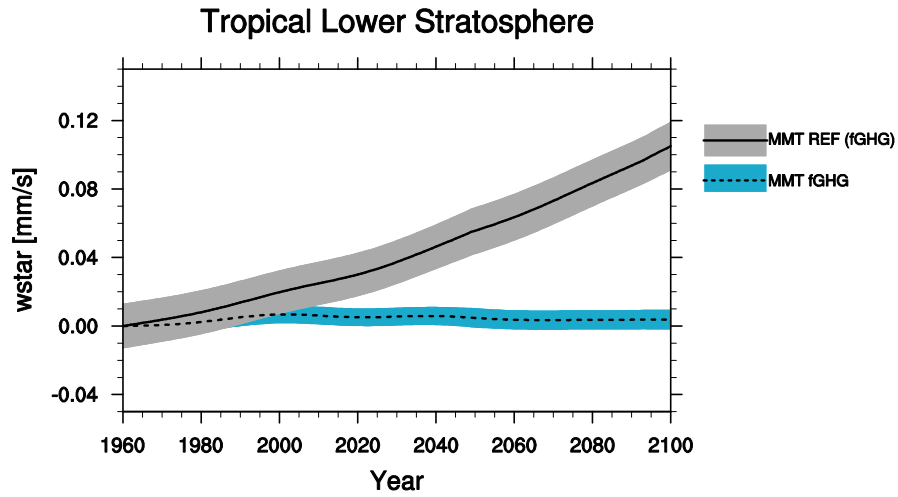


1  
 2 **Figure 9-5:** Multi-model annual mean 90°S-90°N temperature trend from 1980 to 1999 (left panel ),  
 3 and from 2000 to 2099 (right panel). The black line shows the CCMVal-2 multi-model mean and the  
 4 shaded region shows  $\pm 1$  standard deviation about the mean. Multi-model mean derived from Figure 4.4  
 5 of *SPARC CCMVal* (2010).<sup>11</sup>

6  
 7  
 8



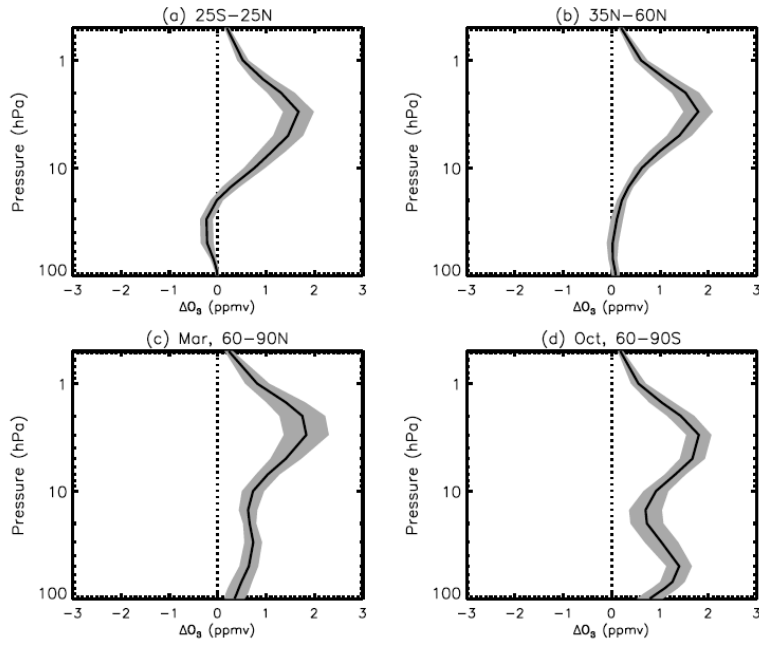
1



2  
3  
4  
5  
6  
7  
8  
9  
10

**Figure 9-6.** Multi-model mean and 95% confidence interval of the 1960 baseline-adjusted annual mean tropical upwelling mass flux between 20°S and 20°N at 70 hPa from the CCMVal-2 reference simulations (MMT REF, solid black line and grey shaded area) and the fixed greenhouse gas simulations (MMT fGHG, black dashed line and blue shaded area). From Figure 5 of *Eyring et al.* [2010].<sup>16</sup>

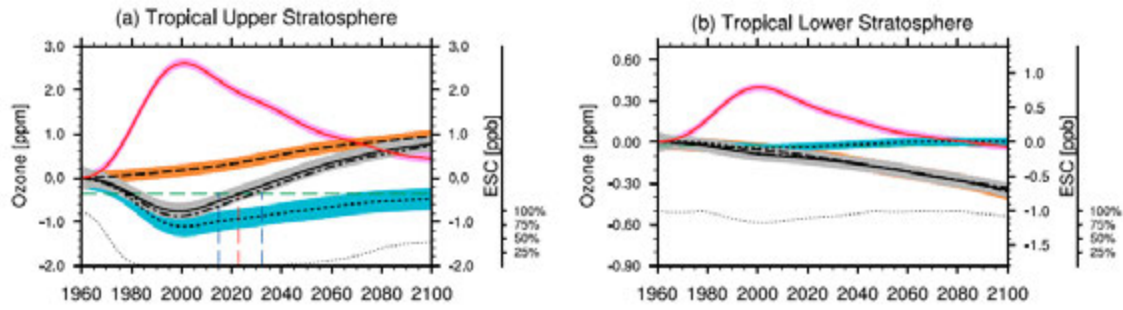
1



2  
3  
4  
5  
6  
7  
8  
9

**Figure 9.7.** Multi-model mean of 2000-2100 ozone changes for different regions. The black line shows the CCMVal-2 multi-model mean and the shaded region shows  $\pm 1$  standard deviation about the mean. Based on analysis in *Oman et al. (2010)*.<sup>18</sup>

1  
2



3  
4



5

6

7

8

9

10

11

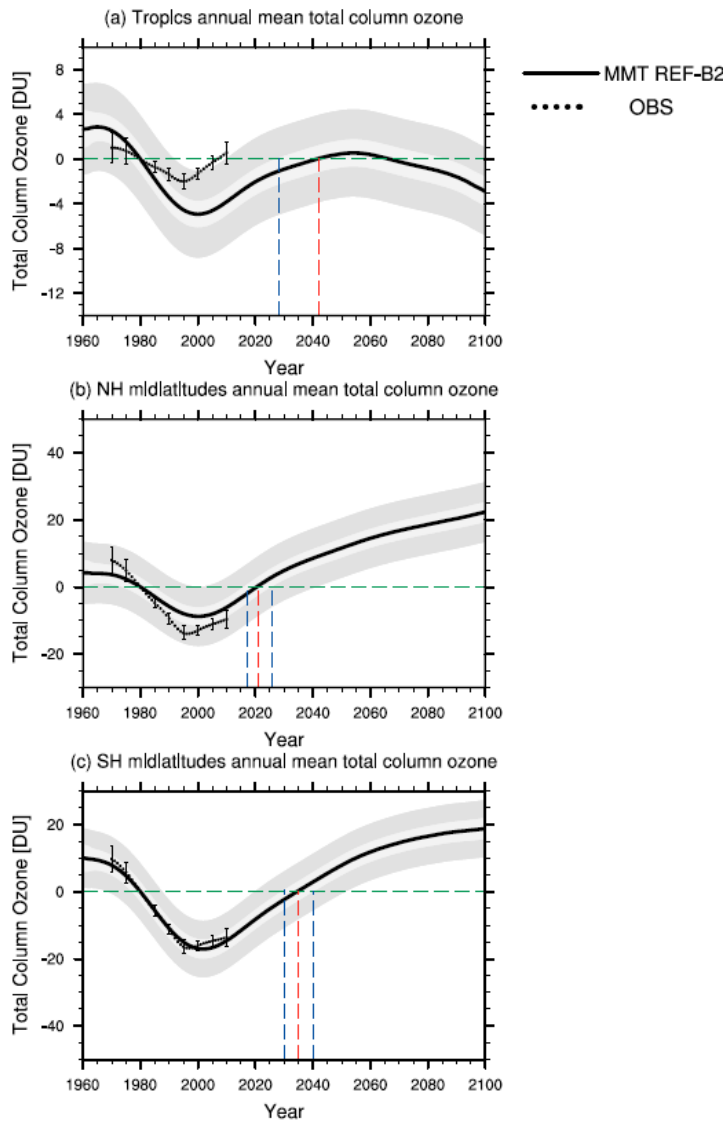
12

13

14

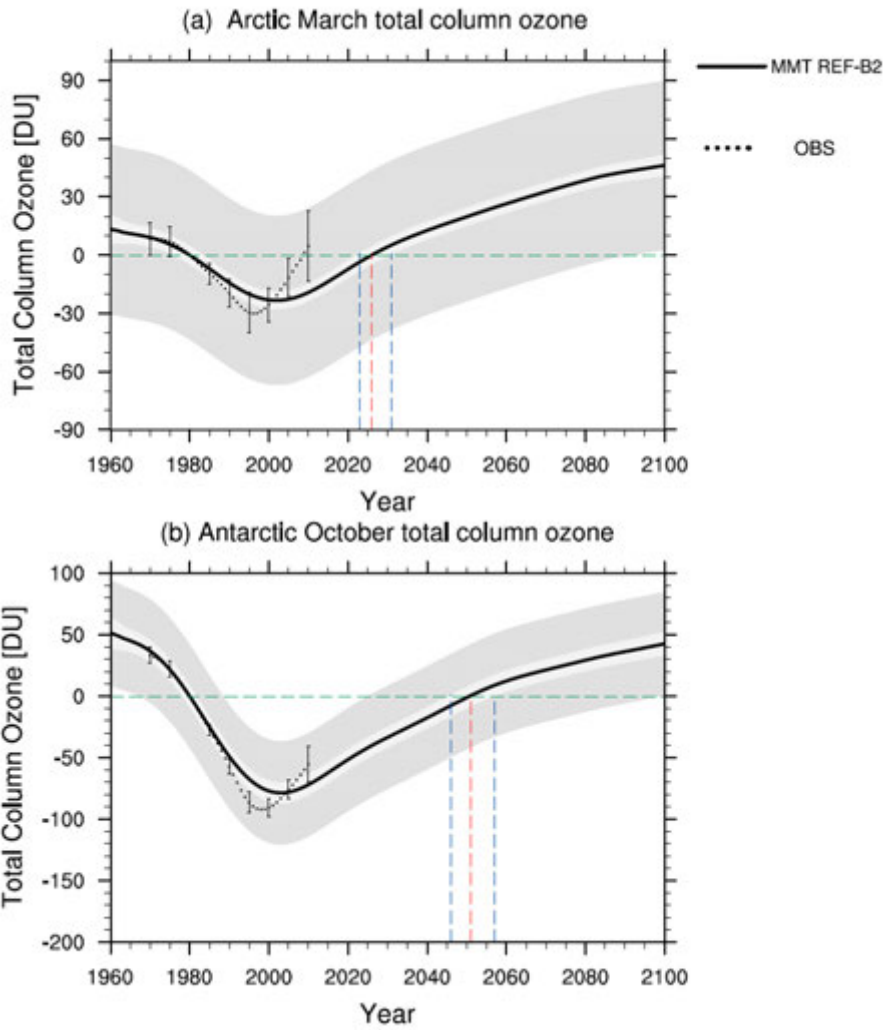
15

**Figure 9.8.** Tropical (25°S-25°N) annual mean 1960 baseline-adjusted ozone projections and 95% confidence for the (a) upper and (b) lower stratosphere. The multi-model trend (MMT) is shown for the CCMVal-2 reference run (REF-B2; black curves and grey shaded area), fixed ODS runs (fODS, black dotted line and orange shaded area), and fixed GHG runs (fGHG, black dashed line and blue shaded area). Also shown is the multi-model trend plus 95% confidence interval for Equivalent Stratospheric Chlorine (ESC), displayed with the red solid line and light red shaded area. See Figure 2 of *Eyring et al.* [2010a] for more details.<sup>16</sup>



1  
2 **Figure 9.9.** 1980 baseline-adjusted multi-model trend estimates of annually averaged total column  
3 ozone (DU) for the tropics (25°S–25°N, upper panel) and midlatitudes (middle panel: 35°N–60°N,  
4 lower panel: 35°S–60°S) (thick dark gray line) with 95% confidence and 95% prediction intervals  
5 appearing as light- and dark-gray shaded regions, respectively, about the trend (note the different  
6 vertical scale among the panels). The red vertical dashed line indicates the year when the multi-model  
7 trend in total column ozone returns to 1980 values and the blue vertical dashed lines indicate the  
8 uncertainty in these return dates. The black dotted lines show observed total column ozone, where a  
9 linear least squares regression model was used to remove the effects of the quasi-biennial oscillation,  
10 solar cycle, El Niño-Southern Oscillation, and volcanoes from four observational data sets. Multi-  
11 model mean derived from Figure 3.6 of *WMO* [2011].<sup>14</sup>  
12  
13

1



2  
3  
4  
5  
6  
7  
8  
9

**Figure 9.10.** As in Figure 9.9, but for the latitude range 60°N–90°N in March (upper row) and the latitude range 60°S–90°S in October (lower row). The red vertical dashed line indicates the year when CCMVal-2 multi-model trend in total column ozone (DU) returns to 1980 values and the blue vertical dashed lines indicate the uncertainty in these return dates. Note the different vertical scale among the panels. Multi-model mean derived from Figure 3.10 of *WMO* [2011].<sup>14</sup>